



Geoenvironmental Application of Novel Persian Gum Biopolymer in Sandy Soil Stabilization

Mohsen Adabi¹ · Ehsan Darvishan² · Gale Eyvazi² · Hila Jahanbaksh Motlagh²

Received: 31 August 2021 / Accepted: 30 January 2022 / Published online: 27 February 2022
© King Fahd University of Petroleum & Minerals 2022

Abstract

Persian gum as a newly introduced hydrocolloid with unique adhesive and gel forming properties has found wide applications in various industries such as medicine, food and textile. Recently, it has been employed in soil environment as a biocompatible stabilizing agent. However, due to its novelty, there is no study about its application in cohesionless sandy soil. This paper provides a comprehensive evaluation of Persian gum treated sand through macro- and microscale tests including compaction, unconfined compressive strength (UCS), direct shear (DS), triaxial (UU), California bearing ratio (CBR), falling head permeability, scanning electron microscopy (SEM), stereo zoom microscopy (SZM), Brunner, Emmet and Teller (BET), particle size analysis (PSA) and thermal gravimetric analysis (TGA). The tests were conducted on untreated and treated soil with different Persian gum contents and curing times. The obtained results represent the powerful performance of this novel gum in mechanical strength and bearing capacity enhancement through binding soil particles and formation of large agglomerated grains. Also, the remarkable ability of this novel gum in pore filling and compacting soil interstructure makes it a favorable additive in soil projects with permeability reduction purposes.

Keywords Persian gum · Soil stabilization · Biopolymer · Sandy soil · Hydrocolloids

1 Introduction

Population growth and rapid construction development has put soil stabilization in the center of attention as one of the most important parts of civil engineering projects. Various techniques of soil improvement can be categorized as mechanical, electrical, chemical and biological methods [1]. Mechanical approach is the oldest and proven method that applies static and dynamic forces to compact the soil layers and increases its density for predetermined objectives. There are numerous studies about application of common mechanical methods such as densification [2], dewatering through consolidation or drainage [3], reinforcement [4], pre-compression [5], stone columns [6], deep mixing [7] and vibroflotation [8]. The mechanical methods are time-consuming and require heavy and expensive equipment with

the capability to produce considerably large forces. Electrical stabilization is another stabilizing method that is also expensive and rarely used [9]. In this method, some metal electrodes are inserted into the soil and the current produced between them enhances soil structure and stabilizes it. Among different techniques that have been applied for soil improvement, chemical soil stabilization is the mostly used approach that employs adhesive property of the additives to enhance interactions between soil particles [10, 11]. The initial soil stabilization materials, known as traditional ones, including lime, cement, fly ash, slag, gypsum and bituminous materials had lots of detrimental effects on the environment such as huge amounts of CO₂ and NO₂ emission in their production process, energy resources depletion, brittle behavior of the soil that leads to structural failure and seismic hazard, increase in pH of soil and vegetation threat [12–14]. To mitigate these undesirable effects, non-traditional additives such as blast furnace slag, resins, ions, acids, silicates, polymers and geopolymers have been developed [15–22]. However, they were not completely successful in elimination of negative environmental impacts due to their cement-dependent and undegradable nature. In an effort to satisfy environmental goals and eliminate the

✉ Ehsan Darvishan
darvishan@riau.ac.ir

¹ Department of Metallurgy and Materials Science, Roudehen Branch, Islamic Azad University, Roudehen, Iran

² Department of Civil Engineering, Roudehen Branch, Islamic Azad University, Roudehen, Iran



whole destructive impacts of soil additives on the environment, biological stabilization using some kinds of living organisms and biomaterials such as enzymes, lignin, chitosan, casein and hydrocolloids (natural gums) has been investigated extensively [23–27]. Hydrocolloids as a kind of biopolymers including xanthan, guar, sodium alginate, gelatin, agar with their considerable gel formation and binding properties have been the subject of many soil stabilization studies in recent years [28–32]. The results have shown their powerful performance in soil strengthening, erosion and permeability reduction. The increasing demand for biocompatible materials on the one hand and the powerful performance of hydrocolloids in soil improvement have encouraged geotechnical engineers to seek new sources of them for soil stabilization.

Persian gum as a kind of biopolymers is one of the novel biocompatible soil additives that has been recently introduced to the soil environment [33]. This novel gum is categorized as plant exudate gums and obtained from branches and trunk of Almond trees scattered in vast areas of arid and semiarid regions of Fars province in Iran. Similar to other kinds of hydrocolloids, this novel source of natural gums has profitable viscosity enhancement, gel formation and adhesive properties that make it favorable to apply in different industries such as food, medicine and textile [34–37]. A recently conducted research has shown its potential performance in clayey soil improvement through binding soil particles together. The comparison between strength results of Persian gum treated soil with other common hydrocolloid treated ones revealed that this novel gum can be used as a powerful substitute for the other conventional hydrocolloids in soil stabilization [33]. The unknown behavior of Persian gum as a newly introduced soil additive has intensified the urgent need for investigation about its effects on different kinds of soil and also different aspects of soil properties.

As well as cohesive soils, Persian gum seems to be a proper choice to improve cohesionless soil due to its prominent adhesive property. On this basis, considering lack of any study about novel Persian gum application on cohesionless soil, this paper was arranged to evaluate geotechnical properties of sandy soil stabilized with Persian gum. A comprehensive set of experiments including compaction, unconfined compressive strength, direct shear, unconsolidated-undrained triaxial, California bearing ratio, permeability, microscopic images, Bruner, Emmet and Teller, particle size analysis and thermogravimetric analysis tests were arranged to fully evaluate the macro- and microscale behavior of the soil. The tests were conducted on soil specimens before and after treatment to discover how Persian gum changes soil properties. Different contents of Persian gum were added to the soil and the results of the tests

Table 1 Soil properties

Engineering and chemical properties	Standard	Values
Unified soil classification system (USCS)	ASTM D2487	SP
Specific gravity (G_s)		2.74
<i>Compaction parameters</i>		
Maximum dry unit weight (MDU) (kN/m^3)	ASTM D1557	16.5
Optimum moisture content (OMC) (%)		16.5
Chemical composition	ASTM D8064	
SiO ₂		95–98%
Al ₂ O ₃		0.5–1.0%
Fe ₂ O ₃		0.5–1.0%
CaO		0.5–1.0%
Na ₂ O		0.02–0.5%
K ₂ O		0.5–0.7%

were employed to determine optimum Persian gum content.

2 Materials

2.1 Soil

The soil employed in the experimental program was sand collected from Firoozkooh region, Tehran, Iran. It was purchased from Maseh Rikhtegari Company in 30 kg bags. The specific gravity of the soil was reported as 2.7 gr/cm^3 . According to the compaction test results [38], maximum dry unit weight and optimum moisture content of the soil were reported as 16.5 kN/m^3 and 16.5%, respectively. The soil was classified as poorly graded sand (SP) considering unified soil classification system (UCSC) classification. The physiochemical properties of the soil are presented in Table 1.

2.2 Persian Gum

Persian gum is a recently introduced polysaccharide that is taken from the branches and trunk of wild Almond trees grown in Zagros jungles of Fars province, Iran [39]. This novel anionic hydrocolloid, classified as exudate plant gums, has many behavioral similarities to well-known Arabic gum. However, some structural characteristics such as xylose and mannose units in its structure, the protein content and the adverse ratio of arabinose to galactose differentiate this gum from its competitor. Mg, Ca, Fe, Zn, Na and K are the divalent and monovalent cations existed in this gum [40]. Chromatographic methods have revealed the main monosaccharides of Persian gum as arabinose and galactose. Also, some other

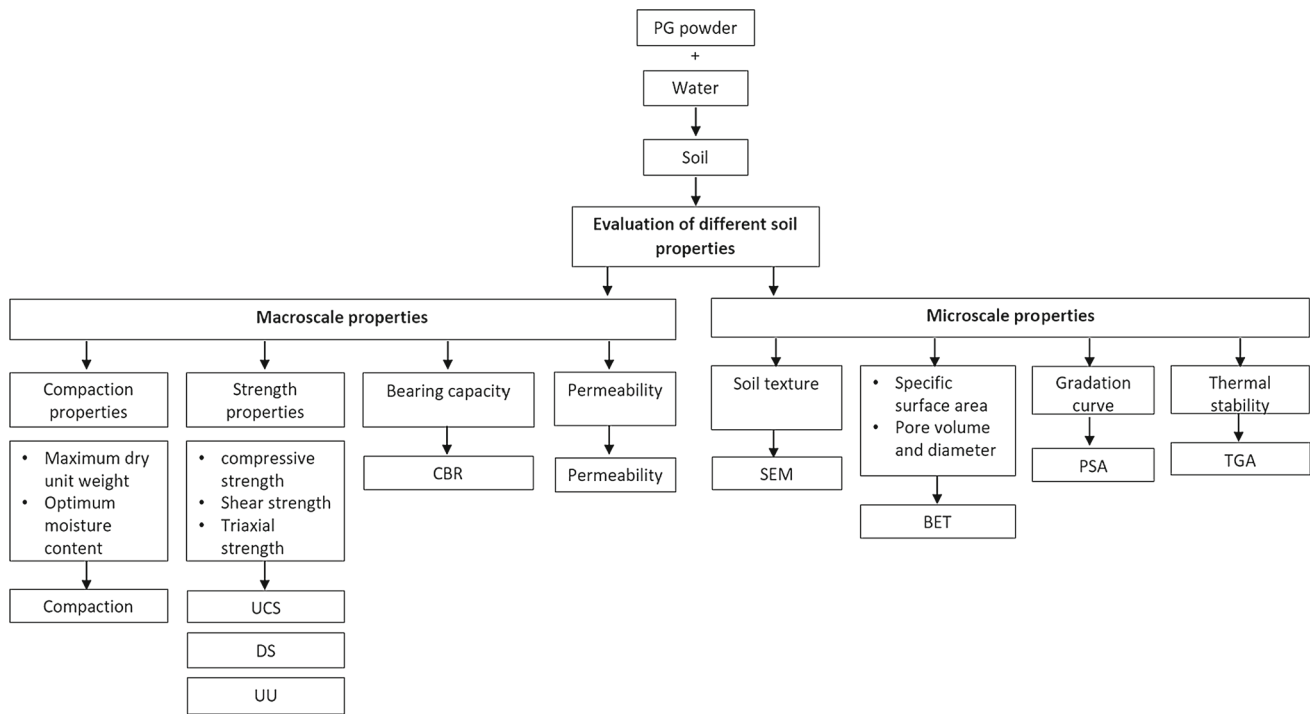
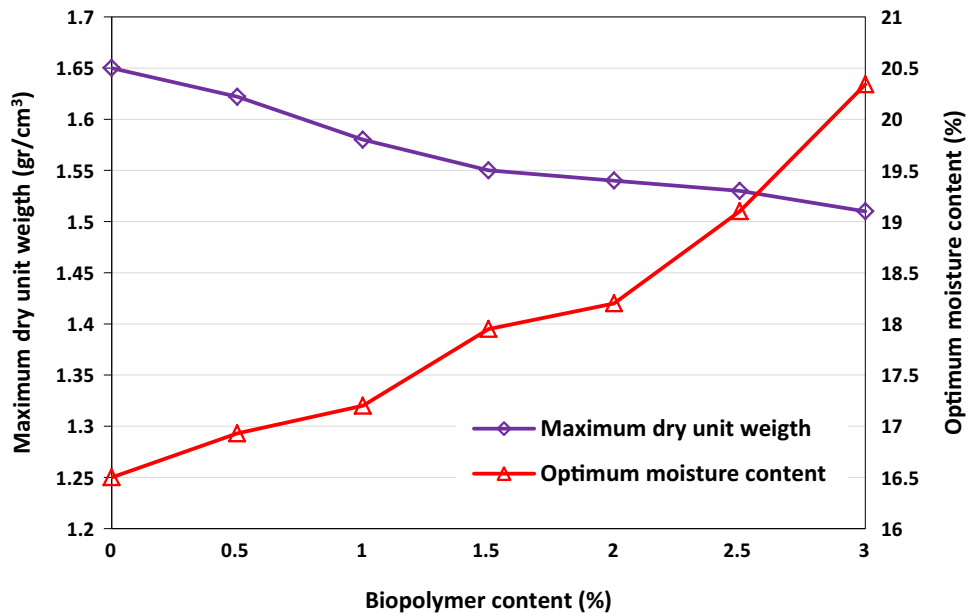


Fig. 1 The methodological scheme of the conducted research

Fig. 2 Compaction characteristics for untreated and treated sand specimens with different contents of Persian gum (0.5, 1, 1.5, 2, 2.5 and 3%)



20 mm to reach to the maximum dry unit weight and taken out by a jack very gently. The specimens were cured at room temperature of 25 °C for 7, 28 and 90 days.

For CBR experiment, the mixture of soil–water–biopolymer was compressed in CBR molds in 3 layers to achieve maximum dry unit weight and optimum water content obtained from compaction tests. The aforementioned percentages of biopolymer were applied to prepare the specimens. To investigate the effect of curing time on CBR values,

the 7, 28 and 90 days treated specimens were exposed to the CBR test.

For permeability test, the specified amounts of biopolymer including 0.5, 1, 1.5, 2, 2.5 and 3% by weight of dry soil, water and oven-dried soil were mixed and compressed in a mold of 68 mm diameter and 50 mm height to reach the optimum water content and maximum dry unit weight determined from compaction test of each biopolymer treated soil.

For microscale tests, the tiny pieces of crushed specimens after failure were used. For SEM test, a very small piece of crushed sample with flat and clean surface was separated using a tweezer. The carbon studs were coated with a layer of graphite and the soil flakes were carefully placed on them. After drying soil samples for about 5 min at the room temperature, they were placed in the testing platform of SEM chamber for sputter coating. A 10-nm gold layer was used to coat the samples and the thickness of the coating was measured using a touch screen control. After the coating process was completed, the samples were removed from the sputter coater and placed in a dish to be ready for transformation in SEM device. Since fine-grained soils are considered as more sensitive kind of soils, the correct selection of the specimen size for SEM test is of great importance. The dimensions of the tiny specimen were selected in a way that it could be accommodated in the SEM chamber easily. For SZM images, no special sample preparation is needed. The images were taken from the cross section of UCS specimens. To conduct BET test on the specimens, the powder form of the specimen was used and degassed under 120 °C temperature for about 3 h. The PSA test was conducted under wet mode in which the powder specimen was dispersed into the water. For TGA test, about 20 mg of powder specimen is needed. The minimal requirements for sample preparation in TGA test are one of the main advantages of this material characterization approach that makes it inexpensive. To conduct the test, a small piece of each crushed specimen was powdered and placed in the platinum crucible and then exposed to the temperature increment from 0 to 800 °C. To evaluate the water content of the specimens by TGA, they were covered with plastic bags to prevent water evaporation. The heating temperature of 100 °C was exposed to the specimens for about 15 min to ensure the complete movement of the water from them. This is advantageous for exact determination of dehydration points. Then, the heating was continued up to 900 °C with the rate of 10 °C/min [46, 47] to obtain initial decomposition and final residue points.

To differentiate the specimens, a specified labeling was applied. The first part of labeling denotes the soil type (S for sandy soil). The second part is related to the treatment condition of the specimens. For untreated sample, the UNT is used as the abbreviation for “untreated” and for treated samples, the biopolymer name and concentration is used to describe the treatment information. For instance, SPG2.5 is referred to the treated sandy soil with 2.5% Persian gum.

4 Testing Program

The UCS test was conducted according to the ASTM D2166 [48]. The strain increment rate was considered to be 1%. The obtained stress strain curves were used to determine the

maximum strength endured by the specimens. After failure, the small pieces of crushed specimens were put in the oven to calculate moisture content of the soil.

Direct shear test was conducted in accordance with ASTM D3080 [49] on the treated soil samples. The cured samples were put in the shear box with strain rate of 0.8 mm/min until the specimens failed or experienced 10 mm displacement. Three normal stresses of 100, 200 and 300 kPa were applied on each specimen. Considering normal and shear stresses, failure envelope was plotted and shear parameters including cohesion and angle of friction were obtained.

The samples were exposed to UU test according to the ASTM D2850 [50] to achieve shear parameters of treated soil under confining pressure of 100, 200 and 300 kPa.

CBR test was conducted according to the ASTM D1883 [51] to evaluate the effect of biopolymers on bearing capacity of the soil. The penetrations of 2.5 and 5 mm were applied for the test.

To measure permeability of the specimens, the pure and 7 days treated sand were saturated in water and the falling head permeability test was conducted according to the ASTM D5084 [52]. Three identical specimens were exposed to the test and the average result was considered as the coefficient of permeability.

SEM as a kind of powerful identification method was applied to characterize soil microstructure. The electron beam was focused to the sample surface and interacted with it. The reflected rays were characterized and converted to the signals to generate microscopic images. SZM is the other way for providing microscopic images. In this optical method, the reflected light from the surface of the sample is used to produce images. Motic stereo zoom microscope with strong zoom property is used to provide images of untreated and treated soil specimens. BET test is the other material characterization method that provides useful information about specific surface area, pore volume and distribution of soil particles. Nitrogen gas adsorbate was injected to the sample cell and its pressure was altered under constant temperature. After development of gas distribution model and BET equation, specific surface area was calculated. The total absorbed gas at 1 atm and 77 °K was introduced as the pore volume of the soil medium. To obtain precise gradation curve of soil samples, PSA test was conducted using Sympatec Helos and Cavette laser diffractometer. The laser light was radiated to the specimen and the reflected light was measured in terms of intensity and angle through photodetectors. Fraunhofer theory was applied to analyze data and calculate size of particles. To evaluate thermal behavior of the specimens, TGA tests were conducted using Mettler-Toledo setup. The samples were heated from 0 to 800 °C, and the heating rate was adjusted to 10 °C/min.

The methodological scheme of the research is shown Fig. 1.

5 Results and Discussion

5.1 Compaction

Compaction characteristics determination is of great importance, since such characteristics directly affect other mechanical aspects of soil behavior such as soil strength, bearing capacity, permeability and settlement. To discover these important soil properties including maximum dry unit weight and optimum moisture content, compaction tests were conducted on the soil specimens with different biopolymer contents. As it can be seen in Fig. 2, the increase in biopolymer concentration from 0 to 2.5% leads to the decrease in maximum dry unit weight from 1.65 to 1.51 gr/cm³. This can be related to the soil particle weights and also biopolymer solution viscosities [53]. Since the used soil particles have low weight, the easy movement of them caused by viscose hydrogels is possible. With the increase in biopolymer content, viscosity of the formed hydrogels is improved [54]. Therefore, as biopolymer content increases, the soil particles move easier on each other and more reduced dry unit weight is obtained.

Optimum moisture content as the other important compaction characteristic of the soil was found to be increased with the addition of biopolymer. The amount of this parameter grows from 16.5 to 20.3% by increasing biopolymer content from 0 to 3%. This is expected considering the hydrophilic nature of the Persian gum, as a kind of hydrocolloids, that causes more water absorption [55].

5.2 Unconfined Compressive Strength

5.2.1 Optimization

Different contents of Persian gum including 0.5, 1, 1.5, 2, 2.5 and 3% of dry soil weight were used to treat sandy soil and the 7 days treated samples were exposed to the UCS test. Figure 3a represents the results of UCS tests for treated soils with different biopolymer contents. According to the results, the UCS of treated soil samples including SPG0.5, SPG1, SPG1.5, SPG2, SPG2.5 and SPG3 is 73.7, 232, 540, 699.6, 782.8 and 675 kPa, respectively. These UCS values induced for sand samples as a kind of cohesionless soil are considerable. The reason is related to the powerful binding property of Persian gum hydrogels that connect soil particles together through connection bridges. Furthermore, the branched structure of PG [41], high molecular weight [56] and existence of various functional groups in the structure of Persian gum (revealed from its FTIR spectrum) [40] facilitate its interaction with soil particles. The abundance of carboxyl and hydroxyl groups in the chemical structure of Persian gum provides lots of potential connection spaces for binding to the soil particles. This can be the reason for powerful adhesive

property of the hydrogel additives. The adhesive film strands between soil particles cause formation of agglomerated particles in the soil medium that resist against transitional and rotational motions in the specimen induced by external forces [57]. The values of unconfined compressive strength of soil specimens grew with the increase in biopolymer content. This fact is expected, as the number of formed bonds and interactions has been improved by higher biopolymer content. However, at a specified level of the biopolymer, the compressive strength started to decrease. This can be due to the overcoming lubricating role of the formed hydrogels to their adhesive property that causes soil grains move freely on each other and decreases soil overall strength [58]. This increasing and decreasing trend of strength variations with biopolymer content is similar for the soil treated with other kinds of biopolymers [59]. The polymer content related to the maximum compressive strength is introduced as optimum biopolymer content. Therefore, 2.5% Persian gum is considered as the optimum biopolymer level for sandy soil treatment. Occurrence of maximum compressive strength at this biopolymer content reveals formation of powerful gel network for Persian gum hydrogels that resist against applied forces.

5.2.2 Curing Time

To investigate the effect of curing time as an important parameter for soil stabilization projects, the optimum Persian gum treated sample was cured at room temperature of 25 °C for various curing times of 3, 7, 14, 28 and 90 days. The results of UCS tests are recorded and shown in Fig. 3b. As it can be seen, the maximum strength of optimum Persian gum treated soil cured at 3, 7, 14, 28 and 90 days of curing is 350, 782, 1096, 1286 and 1390 kPa, respectively. The growth of strength with time is related to the formation of new bonds and completion of formed ones during the time. Dehydration of soil specimens over time is the other reason for increase in soil strength [60]. According to the gel properties, Persian gum hydrogels show the more powerful adhesive properties when losing water [61]. The strength of 3, 7, 14, 28 days treated specimens is 0.25, 0.56, 0.79 and 0.93% of 90 days cured sand. As the results show, after 28 days of curing, the increment of strength is negligible. This shows that most of the interactions have been completed till 28 days and there is not any major chemical interaction between soil particles and biopolymer hydrogels after 28 days of curing.

5.3 Direct Shear Test

To evaluate shear performance of Persian gum stabilized soil considering various polymer contents and curing times, direct shear tests were conducted on SPG0.5, SPG1, SPG1.5, SPG2, SPG2.5, SPG3 at various curing times of 7, 28 and

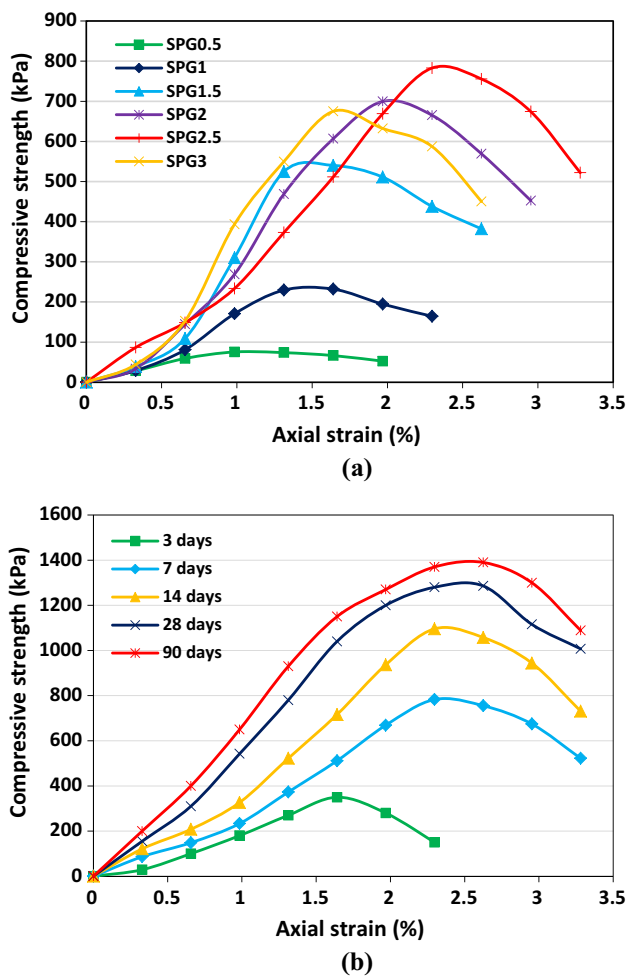


Fig. 3 Unconfined compressive strength test results for a 7 days treated sand specimens with different contents of Persian gum (0.5, 1, 1.5, 2, 2.5 and 3%) **b** Optimum treated sand specimen at different curing times (3, 7, 14, 28 and 90 days)

90 days. The results of shear parameters including cohesion and friction angle for treated sand specimens are shown in Fig. 4. As it can be seen, for all curing times, the increase in biopolymer content has led to the improvement of cohesion parameter and reduction of friction angle. In sandy soil, there is very limited cohesion between soil particles and the main resistance of the soil is provided by the internal friction angle between soil particles. Therefore, for sand treated with biopolymer, the induced cohesion is attributed to the cohesion and viscosity of the formed hydrogels [62]. In the treated soil, the interaction between the biopolymer hydrogels and sand particles is weak due to the electrically neutral surface of soil aggregates and the strength of soil–biopolymer admixture is strongly dependent on the strength of Persian gum hydrogels [63]. During stabilization process, the biopolymer solution transforms from liquid to gel phase. The viscoelastic property of the produced hydrogels has close relation to their strength [64]. According to the previous studies, with

the initial water loss in soil sample (up to about 60%), the biopolymer solution is still a weak gel with limited cohesion and viscous property [65]. As the drying process continues, the viscous property of the formed hydrogel appears at a specified water content. The increase in the hydrogel concentration with the continuous water evaporation [66] intensifies the inter-particle connections that results in the growth of strength. The reduction in friction angle can be explained by lubricating effect of the formed hydrogels [58]. Similar to the UCS test results, the cohesion parameter grows with the increase in biopolymer content, reaches to the maximum level at 2.5% Persian gum content and then starts to decrease. As curing time increases, both shear parameters of cohesion and friction angle show more enhanced values. The amount of these two parameters for 7 days cured sand specimens at optimum biopolymer content is 45 kPa and 29.1°. For 28 days treated specimens, the values of these two parameters have been improved to 86 kPa and 32.3°, while for 90 days stabilized ones, cohesion of 92 kPa and friction angle of 33.9° are obtained. The growth of shear parameters with the increase in curing time can be illustrated by the fact that the bonds strengthen during the time [67]. The cohesion of 7 and 28 days cured optimum treated soil specimens is 49% and 93% of 90 days treated specimen, respectively. This means that the completion of bonds and growth of cohesion parameter continue till 28 days and after that only a small increase in cohesion parameter can be identified.

5.4 Triaxial Test

To gain more realistic shear parameters, UU triaxial test was also conducted on the specimens. Figure 5 shows the total stress failure envelope of the 7 days treated specimens. According to the figure, cohesion of the SPG0.5, SPG1, SPG1.5, SPG2, SPG2.5 and SPG 3 is obtained as 11, 50, 65, 94, 125 and 112 kPa, respectively. A remarkable increase in cohesion can be observed for up to 2.5% biopolymer content, while for more biopolymer contents, cohesion appears to diminish. SPG0.5 shows a slight cohesion since the used pure soil is non-cohesive. However, SPG2.5 represents around 10 times growth in cohesion compared to SPG0.5. The less cohesion for SPG3 can be due to the formation of thick gels between the inter-granular pores that weakens particle compositions [68]. Unlike the cohesion, friction angles tend to slightly decrease by addition of biopolymer content. The friction angles for the aforementioned specimens are 35.0, 32.5, 31.3, 29.4, 28.1 and 29.5°, respectively, which show a maximum variations of 5° for 3% change in biopolymer content. As can be observed, the SPG2.5 shows the highest failure envelope. For instance, it shows 178 kPa shear stress for 100 kPa confining pressure that represents 120% growth compared to SPG0.5. As the confining pressures grow, such

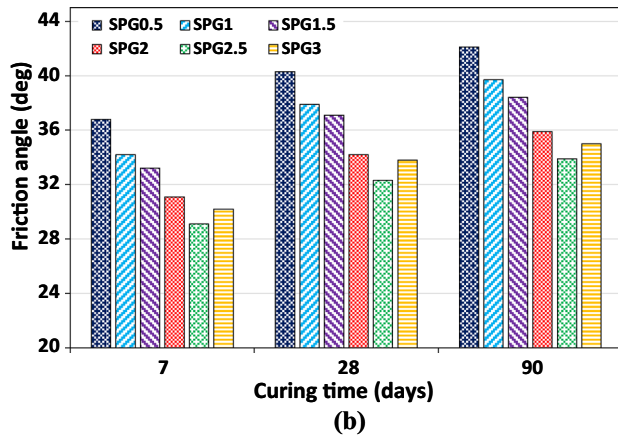
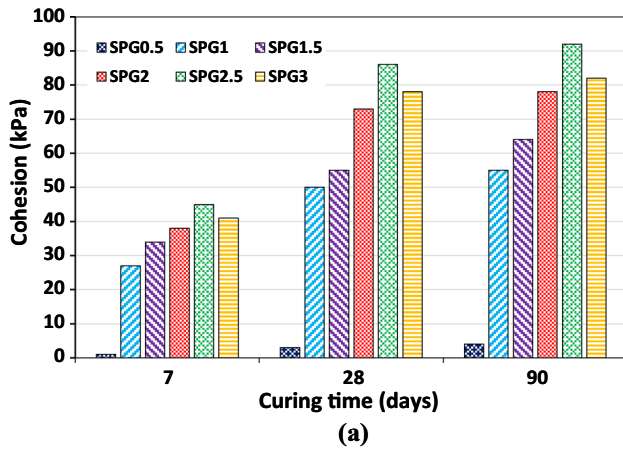


Fig. 4 Direct shear test results of treated sand specimens with different Persian gum contents(0.5, 1, 1.5, 2, 2.5 and 3%) at various curing times of 7, 28 and 90 days: a cohesion b friction angle

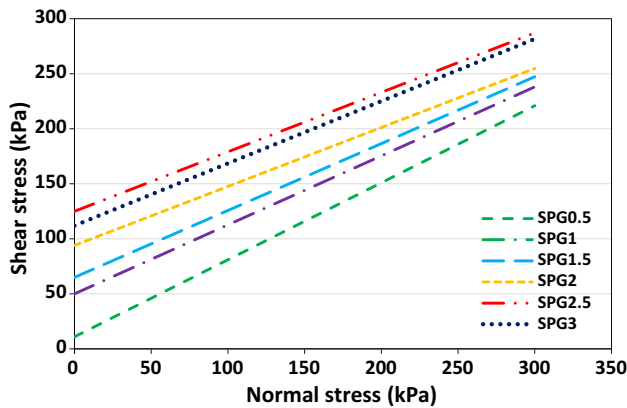


Fig. 5 UU triaxial test results for 7 days treated sand specimens with different contents of Persian gum (0.5, 1, 1.5, 2, 2.5 and 3%)

significant rise in shear strength decreases since the friction angles are reduced with addition of biopolymer content.

Table 3 Bearing capacity of untreated and treated soil with different contents of Persian gum (0.5, 1, 1.5, 2, 2.5 and 3%) and curing times (7, 28 and 90 days)

	Bearing capacity (MPa)					
	CBR 2.5 (mm)			CBR 5.0 (mm)		
	7 days	28 days	90 days	7 days	28 days	90 days
SUNT	3.41	5.81	6.22	3.64	7.26	7.84
SPG0.5	3.54	6.12	6.57	3.82	7.67	8.35
SPG1	4.01	6.74	7.56	4.36	8.60	9.58
SPG1.5	4.63	7.59	8.64	5.90	9.87	11.12
SPG2	7.42	12.56	13.69	9.43	15.89	17.64
SPG2.5	9.10	15.21	16.88	11.90	19.61	21.35
SPG3	8.33	13.77	15.62	10.60	18.04	19.70

5.5 California Bearing Ratio (CBR)

To study the effect of Persian gum on bearing capacity of the soil samples, CBR test was conducted on pure and the treated soil specimens with different biopolymer contents. Table 3 shows the CBR results of SUNT, SPG0.5, SPG1, SPG1.5, SPG2, SPG2.5, SPG3 for 7, 28 and 90 days of curing time. The tests were conducted for two cases of 2.5 and 5 mm penetrations. According to the table, all specimens show higher CBR values (from 6 to about 30%) for 5 mm penetration than 2.5 mm. Therefore, results of 5 mm penetration are discussed hereafter. Generally, treatment with Persian gum causes significant rise in CBR strength. Among the treated specimens, SPG2.5 shows the highest CBR strength of 11.9 for 7 days of curing which is 3.3 times the untreated soil. Therefore, 2.5% is the optimum biopolymer content, considering bearing capacity values. Also, curing time has a sensible effect on CBR values of the specimens. For instance, for SPG2.5 specimen, increase in the curing time from 7 to 28 days causes 65% growth in CBR strength. However, after 28 days of curing, no considerable strength improvement is observed. The 90 days cured SPG2.5 presented only about 9% increase in CBR strength in comparison with the 28 days cured one.

5.6 Permeability Test

Table 4 represents the falling head permeability test results for untreated and treated sand with different amounts of biopolymers. The initial permeability of the pure soil specimen (SUNT) was found to be 1.55×10^{-3} cm/s. For treated specimens including SPG0.5, SPG1, SPG1.5, SPG2, SPG2.5 and SPG3, the coefficient of permeability was reduced to 6.35×10^{-4} , 1.85×10^{-4} , 1.04×10^{-5} , 2.56×10^{-6} , 1.80×10^{-6} and 9.71×10^{-7} cm/s, respectively. As can be observed, higher contents of Persian gum lead to the lower permeability values and the rate of permeability reduction is higher for

Table 4 Permeability test results for treated sand specimens with different contents of Persian gum (0.5, 1, 1.5, 2, 2.5 and 3%)

Biopolymer content (%)	0	0.5	1.0	1.5	2.0	2.5	3
Permeability coefficient (cm/s)	1.55×10^{-3}	6.35×10^{-4}	1.85×10^{-4}	1.04×10^{-5}	2.56×10^{-6}	1.80×10^{-6}	9.71×10^{-7}

lower biopolymer contents. The very low value of hydraulic conductivity for higher amounts of Persian gum (more than 2%) is representative of an impermeable soil layer. Therefore, permeability reduction is a function of biopolymer content. For 0.5% Persian gum, the coefficient of permeability is 40% of the permeability of pure soil. However, for 3% Persian gum, this parameter was reduced to 6% of its value in pure soil. The reduction in permeability of treated soil is due to the formation of viscous hydrogels that are barriers for water flow [69]. The abundance of calcium ion (the gel formation agent of polysaccharides) in the structure of Persian gum enables it to form powerful hydrogels that inhibit water penetration [70]. Previous studies also showed the pore clogging effect of formed hydrogels to reduce soil permeability [71]. With the increase in the biopolymer content, the formed linkages gain volume and swell. These viscose and swelling hydrogels fill more pore spaces and therefore cause more reduction in the soil permeability. The reduction rate of permeability was more considerable at lower biopolymer contents and after a specified level of biopolymer (about 2%), the rate of reduction was reduced. The formed hydrogels give strength to the soil through two mechanisms: 1) pore filling and 2) increase of soil inter-particle interactions [32]. For lower biopolymer contents, pore filling causes the strength growth of the specimen through formation of more compressed structure. For higher biopolymer contents, the interaction role of soil particles and hydrogels is the underlying strength improvement mechanism.

5.7 SEM and SZM Images

SEM images of untreated and treated soil with optimum Persian gum content are shown in Fig. 6a. The formation of adhesive materials is observable in the SEM image of the treated soil. As it can be seen, the formed hydrogels improve soil interstructure through pore filling and formation of connection bridges. In the treatment process, Persian gum biopolymers coagulate and turn into Persian gum films that act as connecting elements between soil aggregates. The prominent calcium ion in the Persian gum chemical structure and the gel producing property of the plant gums [43] can explain the abundance of adhesive hydrogels between treated soil particles. The strengthening mechanism in the interstructure of the optimum treated specimen leads to its mechanical behavior improvement, as observed in the case of other biopolymers such as xanthan, guar, gellan and agar [72–75]. In fact, densification of Persian gum hydrogels

existed in the sand pores through dehydration is the reason for hardening mechanism of sand-Persian gum mixtures. Similar results can be observed from SZM images, as shown in Fig. 6b. It is clear that the treated specimen shows a dense structure in which the inter-particle pores are filled by Persian gum.

5.8 Brunner, Emmet and Teller (BET) Analysis

BET analysis is a powerful technique for material characterization through determination of specific surface area and pore volume, diameter and distribution. These two parameters are important indices for evaluation of soil behavior at microscale. Surface area participates in soil behavior through affecting the interactions between soil particles and adhesive additives. The other influential factor that takes part in soil behavior at microscale is pore volume and diameter, since the variations of these parameters strongly affect the compaction of soil interstructure and therefore alter its behavior. In order to investigate the effect of Persian gum concentration on specific surface area, pore volume, diameter and distribution, BET analysis was conducted on treated sand specimens including SPG0.5, SPG1, SPG1.5, SPG2, SPG2.5 and SPG3. The values of these parameters for treated samples and pore volume distribution are shown in Table 5 and Fig. 7. As the results show, the specific surface area starts to decrease with the increase in biopolymer content. The reason is related to the formation of large agglomerated particles due to the adhesive material that decreases surface area [76]. Considering lower specific surface area as an index of the more effective stabilization, the most reduction of surface area for SPG2.5 verifies it as optimum treated soil sample. The pore volume and mean pore diameter also decrease with the addition of Persian gum. This fact is expected regarding the pore filling property of the formed hydrogels among soil particles. Considering the neural surface of sand particles, the Persian gum hydrogels only fill the pores without any direct interaction with soil particles. This leads to smaller pores with reduced total volume [60]. The diagram of pore distribution, which plots cumulative pore volume against pore diameter, also represents the reduction of pore volume as Persian gum content increases. According to this diagram, 2.5% Persian gum content is the most successful gum concentration in pore volume reduction. This property makes it attractive for soil projects with permeability reduction objectives.



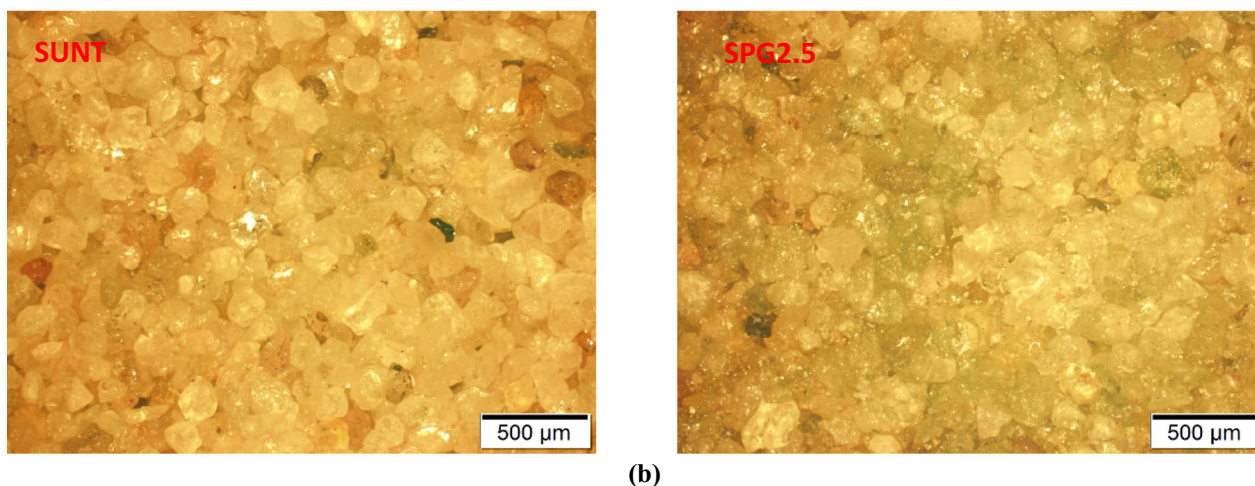
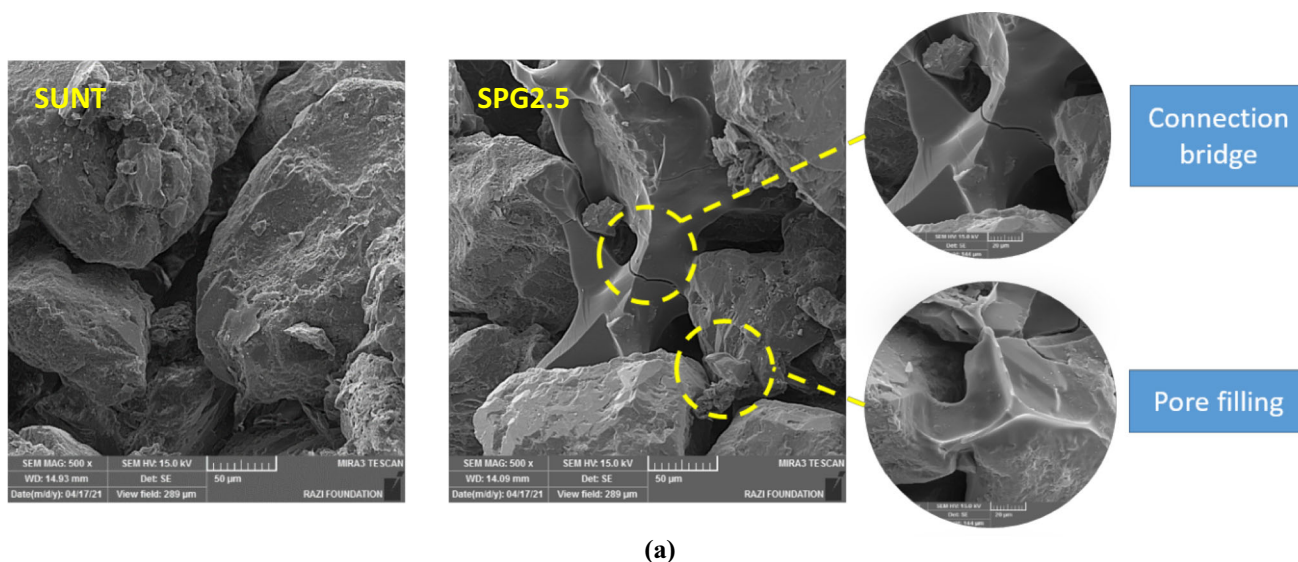


Fig. 6 Microscopic images of untreated and optimum treated specimens a SEM images b SZM images

Table 5 BET test results for treated specimens with different contents of Persian gum (0.5, 1, 1.5, 2, 2.5 and 3%)

	SPG0.5	SPG1	SPG1.5	SPG2	SPG2.5	SPG3
Surface area (m ² /gr)	0.2145	0.2116	0.2040	0.1972	0.1847	0.1968
Pore volume (mm ³ /gr)	1.1090	0.9582	0.7983	0.5958	0.5044	0.5580
Mean pore diameter (nm)	21.746	19.788	14.897	11.887	10.264	11.339

5.9 Particle Size Analysis (PSA)

Soil aggregation is an influential agent on its behavior that can be determined using PSA test. To evaluate the effect of Persian gum concentration on soil gradation curve, PSA tests were conducted on untreated and 7 days treated sand with different contents of Persian gum (0.5, 1, 1.5, 2, 1.5, 2, 2.5 and 3%). According to Fig. 8, with the addition of Persian gum, the gradation curves of treated specimens shift to the right. This is caused by the cementation process that flocculates soil

particles to form large clusters [77]. The S-shaped curves of Persian gum treated samples are related to the size distribution of PG emulsion droplets [34]. The bimodal form of PG size distribution is caused by the insoluble part of this gum that leads to the formation of particles with large sizes [78]. Considering 200, 600 and 1000 μm as the values that distinct fine, medium and coarse grains of sand from each other [79], the optimum Persian gum treated soil is successful in reduction of fine-sized particles of soil from 78 to 39.5%, medium-sized particles from 100 to 82% and coarse-sized

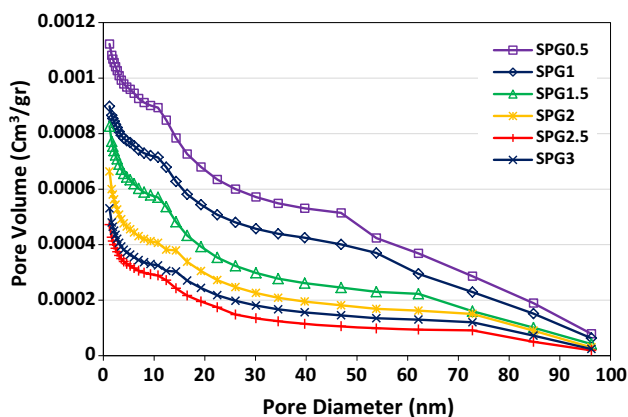


Fig. 7 Pore volume distribution for treated sand specimens with different contents of Persian gum (0.5, 1, 1.5, 2, 2.5 and 3%)

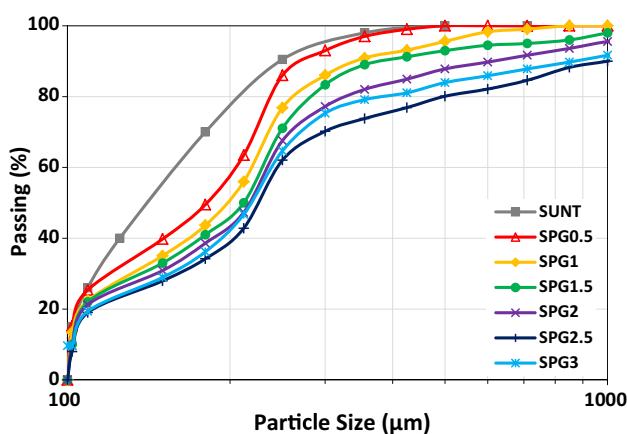


Fig. 8 PSA test results of treated sand specimens with different contents of Persian gum (0.5, 1, 1.5, 2, 2.5 and 3%)

ones from 100 to 89%. This means that optimum Persian gum content can reduce percentage of fine-graded particles of soil to 49.3%. Also, for optimum treated soil, 18% of soil particles are larger than 600 µm and the sizes of 11% of them are beyond 1000 µm, while the untreated soil has no particles larger than 600 µm. The most effective role of the optimum Persian gum in emergence of large agglomerated particles is the basis for its elevated performance in pore filling and binding soil particles, as demonstrated by BET and SEM.

5.9.1 Thermal Gravimetric Analysis (TGA)

TGA tests were conducted on the untreated and treated specimens to investigate their thermal behavior. The thermogravimetric curves of pure and treated soil with different contents of Persian gum are demonstrated in Fig. 9. As it is shown, at a specified temperature, the treated specimens show more weight loss in comparison with the untreated soil. The amount of weight loss increases with the growth of Persian gum content. This is due to the high water retention capac-

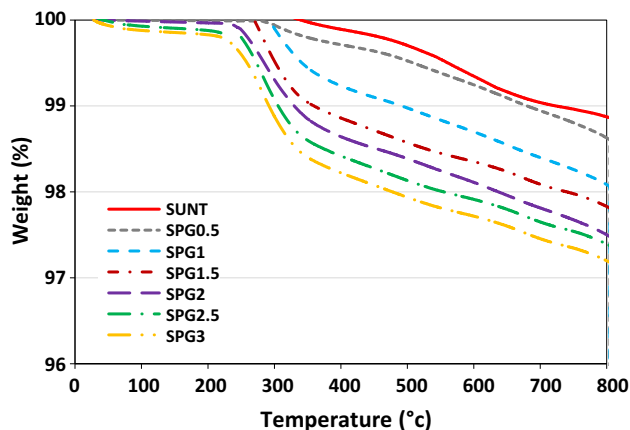


Fig. 9 TGA test results for untreated and treated sand specimens with different contents of Persian gum (0.5, 1, 1.5, 2, 2.5 and 3%)

ity of treated samples with more biopolymer contents due to the lots of hydrophilic functional groups in the structure of gums. Loss of water is the main reason of weight loss before 120 °C. Unlike the fine-grained soils that lose about 20% of their weight at 120 °C [33, 80], the untreated sand has no weight loss before 120°C. This is related to the easy drainage and absence of any surface water in the sandy soil [81]. However, for the treated soil with 2.5 and 3% biopolymer, a slight decrease of 0.1 and 0.15% in the weight of specimens at 120 °C can be observed. This is due to the formation of 3D polymeric networks that trap water inside themselves [82]. In all treated specimens, the observable decrease in weight loss at the range of 350–800 °C can be related to the fugacious organic combinations and lots of hydroxyl groups existed in the soil–biopolymer mixture. In general, the overall weight loss of the treated specimens, when heating from 0 to 800 °C, is found to be very low (about 2%). This is due to the very tiny percentages of added Persian gum. In terms of thermal stability, initial decomposition points (IDT) are appropriate indices [83]. IDT value is the temperature related to the collision point of two tangent lines around the point in which the slope variation is considerable. Conductive research on the TGA and DSC analysis of pure Persian gum determined its IDT as about 250 to 300 °C [43]. As Fig. 9 shows, the value of IDT points for SPG2.5 specimen as the optimum treated sample is 250 °C that is approximately in the same range of Persian gum. According to a previous study, the interactions and cross-links between the biopolymer and negatively charged clayey soil particles cause the IDT point of pure PG to be improved for soil–biopolymer mixtures [33]. However, in the case of sandy soil, as the results show, there are not sufficient cross-links that cause IDT value enhancement.

6 Conclusions

An experimental study was conducted to evaluate effectiveness of recently introduced Persian gum biopolymer on

sandy soil stabilization. The testing program was focused on compaction, strength, bearing capacity and permeability characteristics of the soil. Furthermore, to evaluate the underlying mechanism of mechanical behavior improvement of the soil, a group of microscale tests were conducted. The unconfined compressive strength test results indicated that 2.5% Persian gum by weight of dry soil can be introduced as the optimum biopolymer content for stabilization process. The optimum treated sand specimens represent unconfined compressive strength of 1286 kPa the cohesion parameter of 86 kPa at 28 days of curing and triaxial shear stress of 178 kPa at 7 days of curing. Also, the CBR results show that the bearing capacity of the 7 days optimum treated specimen is 2.7 times the pure soil. Such an improvement in strength and bearing capacity of a cohesionless soil at this low biopolymer content is a great achievement. Also, the remarkable decrease in soil permeability to about 99% using the optimum biopolymer content makes this novel gum favorable for soil projects like seepage barriers and slurry walls, in which low permeability is advantageous. The effect of curing time was investigated through unconfined compressive strength, direct shear test and California bearing ratio tests. According to the results, the most increment in strength and bearing capacity of treated specimens was occurred after 28 days of curing and after that, only a slight increase in the results can be observed. This was related to the formation and completion of most of the interactions and bonds in the interstructure of soil–biopolymer mixture during 28 days of curing. At microscale, the microscopic images represented the positive effect of the used biopolymer on the soil interstructure improvement. The results of BET test revealed that the most reduction of specific surface area and pore volume occurred at optimum Persian gum content. The variations in soil gradation curve obtained from PSA test also confirmed formation of large agglomerated particles in optimum treated soil. Thermal analysis of the specimens indicated more water absorption of soil samples with the increase in biopolymer content that leads to the more weight loss of the specimen when it is exposed to heating.

6.1 Further Research

The enhanced mechanical behavior of cohesionless sandy soil using Persian gum, demonstrated by various macro and microscale tests, proved its beneficial role in soil stabilization. However, due the novelty of this biocompatible additive in the soil stabilization area, further research is required to provide evidence of its effectiveness in field applications. For this purpose, advanced testing program including cyclic triaxial, fatigue, liquefaction and large-scale direct shear tests is needed to be conducted. Investigation about the durability of Persian gum treated soil against environmental conditions such as wet dry and freeze thaw cycles is the other neces-

sity to make this gum applicable in soil projects. Treatment of contaminated soil mediums with Persian gum also is recommended to be the subject of research in order to discover feasibility and effectiveness of Persian gum soil stabilizer in the presence of various contaminants. Considering the purifying effect of some hydrocolloids, the required tests should be conducted to discover the contaminant purifying potential of Persian gum in contaminated soils.

Funding Not applicable.

Data Availability Not applicable.

Code Availability Not applicable.

Declarations

Conflicts of interest Not applicable.

References

- Phummiphan, I.; Horpibulsuk, S.; Rachan, R.; Arulrajah, A.; Shen, S.L.; Chindapasirt, P.: High calcium fly ash geopolymer stabilized lateritic soil and granulated blast furnace slag blends as a pavement base material. *J. Hazard. Mater.* **341**, 257–267 (2018). <https://doi.org/10.1016/J.JHAZMAT.2017.07.067>
- Horpibulsuk, S.; Katkan, W.; Naramitkornburee, A.: Modified Ohio's curves: a rapid estimation of compaction curves for coarse- and fine-grained soils. *Geotech. Test. J.* **32**, 64–75 (2009). <https://doi.org/10.1520/GTJ101659>
- Wu, H.N.; Shen, S.L.; Ma, L.; Yin, Z.Y.; Horpibulsuk, S.: Evaluation of the strength increase of marine clay under staged embankment loading: a case study. *Mar. Georesources Geotechnol.* **33**, 532–541 (2015). <https://doi.org/10.1080/1064119X.2014.954180>
- Sukmak, K.; Sukmak, P.; Horpibulsuk, S.; Han, J.; Shen, S.L.; Arulrajah, A.: Effect of fine content on the pullout resistance mechanism of bearing reinforcement embedded in cohesive-frictional soils. *Geotext. Geomembranes.* **43**, 107–117 (2015). <https://doi.org/10.1016/j.geotextmem.2014.11.010>
- Kafodya, I.; Okonta, F.: Effects of natural fiber inclusions and pre-compression on the strength properties of lime-fly ash stabilised soil. *Constr. Build. Mater.* **170**, 737–746 (2018). <https://doi.org/10.1016/J.CONBUILDMAT.2018.02.194>
- Yoo, C.; Abbas, Q.: Laboratory investigation of the behavior of a geosynthetic encased stone column in sand under cyclic loading. *Geotext. Geomembranes.* **48**, 431–442 (2020). <https://doi.org/10.1016/J.GEOTEXMEM.2020.02.002>
- Bo, M.W.; Arulrajah, A.; Choa, V.; Horpibulsuk, S.; Disfani, M.M.: Deep compaction of granular fills in a land reclamation project by dynamic and vibratory compaction techniques. In: *Ground Improvement Case Histories: Compaction, Grouting and Geosynthetics*. pp. 263–274 (2015)
- BaBachowski, L.: Vibroflotation Control of Sandy Soils using DMT and CPTU. Presented at the (2015)
- Winterkorn, H.F.; Pamukcu, S.: Soil stabilization and grouting. *Found. Eng. Handb.* (1991). https://doi.org/10.1007/978-1-4757-5271-7_9

10. Behnood, A.: Soil and clay stabilization with calcium- and non-calcium-based additives: a state-of-the-art review of challenges, approaches and techniques. *Transp. Geotech.* **17**, 14–32 (2018). <https://doi.org/10.1016/j.trgeo.2018.08.002>
11. Firoozi, A.A.; Guney Olgun, C.; Firoozi, A.A.; Baghini, M.S.: Fundamentals of soil stabilization. *Int. J. Geo-Engineering.* **8**, 1–16 (2017). <https://doi.org/10.1186/s40703-017-0064-9>
12. Ikeagwuani, C.C.; Nwonu, D.C.: Emerging trends in expansive soil stabilisation: a review. *J. Rock Mech. Geotech. Eng.* **11**, 423–440 (2019). <https://doi.org/10.1016/J.JRMGE.2018.08.013>
13. Fasihnikoutalab, M.H.; Asadi, A.; Kim Huat, B.; Westgate, P.; Ball, R.J.; Pourakbar, S.: Laboratory-scale model of carbon dioxide deposition for soil stabilisation. *J. Rock Mech. Geotech. Eng.* **8**, 178–186 (2016). <https://doi.org/10.1016/j.jrmge.2015.11.001>
14. Yi, Y.L.; Liska, M.; Unluer, C.; Al-Tabbaa, A.: Initial investigation into the carbonation of MgO for soil stabilisation. In: 18th International Conference on Soil Mechanics and Geotechnical Engineering: Challenges and Innovations in Geotechnics, ICSMGE 2013. pp. 2641–2644. IOS Press (2013)
15. Ogila, W.A.M.: Effectiveness of fresh cement kiln dust as a soil stabilizer and stabilization mechanism of high swelling clays. *Environ. Earth Sci.* **80**, 283 (2021). <https://doi.org/10.1007/s12665-021-09589-4>
16. Jiang, N.J.; Du, Y.J.; Liu, K.: Durability of lightweight alkali-activated ground granulated blast furnace slag (GGBS) stabilized clayey soils subjected to sulfate attack. *Appl. Clay Sci.* **161**, 70–75 (2018). <https://doi.org/10.1016/j.clay.2018.04.014>
17. Hamidi, S.; Marandi, S.M.: Clay concrete and effect of clay minerals types on stabilized soft clay soils by epoxy resin. *Appl. Clay Sci.* **151**, 92–101 (2018). <https://doi.org/10.1016/j.clay.2017.10.010>
18. Tingle, J.S.; Newman, J.K.; Larson, S.L.; Weiss, C.A.; Rushing, J.F.: Stabilization mechanisms of nontraditional additives. *Transp. Res. Rec.* **2**, 59–67 (2007). <https://doi.org/10.3141/1989-49>
19. Jayanthi, P.N.V.; Singh, D.N.: Utilization of sustainable materials for soil stabilization: state-of-the-art. *Adv. Civ. Eng. Mater.* **5**, 20150013 (2016). <https://doi.org/10.1520/ACEM20150013>
20. Ghasemzadeh, H.; Mehrpajouh, A.; Pishvaei, M.; Mirzababaei, M.: Effects of curing method and glass transition temperature on the unconfined compressive strength of acrylic liquid polymer-stabilized kaolinite. *J. Mater. Civ. Eng.* **32**, 04020212 (2020). [https://doi.org/10.1061/\(asce\)mt.1943-5533.0003287](https://doi.org/10.1061/(asce)mt.1943-5533.0003287)
21. Khadka, S.D.; Jayawickrama, P.W.; Senadheera, S.; Segvic, B.: Stabilization of highly expansive soils containing sulfate using metakaolin and fly ash based geopolymer modified with lime and gypsum. *Transp. Geotech.* **23**, 100327 (2020). <https://doi.org/10.1016/j.trgeo.2020.100327>
22. Chen, R.; Zhu, Y.; Lai, H.P.; Bao, W.: Stabilization of soft soil using low-carbon alkali-activated binder. *Environ. Earth Sci.* **79**, 510 (2020). <https://doi.org/10.1007/s12665-020-09259-x>
23. Almajed, A.; Abbas, H.; Arab, M.; Alsabhan, A.; Hamid, W.; Al-Salloum, Y.: Enzyme-induced carbonate precipitation (EICP)-based methods for ecofriendly stabilization of different types of natural sands. *J. Clean. Prod.* **274**, 122627 (2020). <https://doi.org/10.1016/j.jclepro.2020.122627>
24. Zhang, T.; Cai, G.; Liu, S.: Application of lignin-stabilized silty soil in highway subgrade: a macroscale laboratory study. *J. Mater. Civ. Eng.* **30**, 04018034 (2018). [https://doi.org/10.1061/\(asce\)mt.1943-5533.0002203](https://doi.org/10.1061/(asce)mt.1943-5533.0002203)
25. Hataf, N.; Ghadir, P.; Ranjbar, N.: Investigation of soil stabilization using chitosan biopolymer. *J. Clean. Prod.* **170**, 1493–1500 (2018). <https://doi.org/10.1016/j.jclepro.2017.09.256>
26. Fatehi, H.; Abtahi, S.M.; Hashemolhosseini, H.; Hejazi, S.M.: A novel study on using protein based biopolymers in soil strengthening. *Constr. Build. Mater.* **167**, 813–821 (2018). <https://doi.org/10.1016/j.conbuildmat.2018.02.028>
27. Anandha Kumar, S.; Sujatha, E.R.: Compaction and Permeability Characteristics of Biopolymer-Treated Soil. In: *Lecture Notes in Civil Engineering*. pp. 107–117. Springer Science and Business Media Deutschland GmbH (2021)
28. Moghal, A.A.B.; Vydehi, K.V.: State-of-the-art review on efficacy of xanthan gum and guar gum inclusion on the engineering behavior of soils. *Innov. Infrastruct. Solut.* **6**, 1–14 (2021). <https://doi.org/10.1007/s41062-021-00462-8>
29. Fatehi, H.; Bahmani, M.; Noorzad, A.: Strengthening of dune sand with sodium alginate biopolymer. In: *Eighth International Conference on Case Histories in Geotechnical Engineering (Geo-Congress 2019)*, pp. 157–166. American Society of Civil Engineers (ASCE) (2019)
30. Chang, I.; Im, J.; Lee, S.W.; Cho, G.C.: Strength durability of gelatin gum biopolymer-treated Korean sand with cyclic wetting and drying. *Constr. Build. Mater.* **143**, 210–221 (2017). <https://doi.org/10.1016/j.conbuildmat.2017.02.061>
31. Smitha, S.; Rangaswamy, K.; Keerthi, D.S.: Triaxial test behaviour of silty sands treated with agar biopolymer. *Int. J. Geotech. Eng.* **15**, 484–495 (2021). <https://doi.org/10.1080/19386362.2019.1679441>
32. Cabalar, A.F.; Awraheem, M.H.; Khalaf, M.M.: Geotechnical properties of a low-plasticity clay with biopolymer. *J. Mater. Civ. Eng.* **30**, 04018170 (2018). [https://doi.org/10.1061/\(ASCE\)MT.1943-5533.0002380](https://doi.org/10.1061/(ASCE)MT.1943-5533.0002380)
33. Ghasemzadeh, H.; Modiri, F.: Application of novel Persian gum hydrocolloid in soil stabilization. *Carbohydr. Polym.* (2020). <https://doi.org/10.1016/j.carbpol.2020.116639>
34. Golkar, A.; Taghavi, S.M.; Dehnavi, F.A.: The emulsifying properties of persian gum (*Amygdalus scoparia* spach) as compared with gum arabic. *Int. J. Food Prop.* **21**, 416–436 (2018). <https://doi.org/10.1080/10942912.2018.1454464>
35. Sadeghi, F.; Kadkhodae, R.; Emadzadeh, B.; Phillips, G.O.: Phase behavior, rheological characteristics and microstructure of sodium caseinate-Persian gum system. *Carbohydr. Polym.* **179**, 71–78 (2018). <https://doi.org/10.1016/j.carbpol.2017.09.060>
36. Raoufi, N.; Kadkhodae, R.; Fang, Y.; Phillips, G.O.: Ultrasonic degradation of Persian gum and gum tragacanth: effect on chain conformation and molecular properties. *Ultrasound. Sonochem.* **52**, 311–317 (2019). <https://doi.org/10.1016/j.ulsonch.2018.12.002>
37. Mohammadi, S.; Abbasi, S.; Scanlon, M.G.: Development of emulsifying property in Persian gum using octenyl succinic anhydride (OSA). *Int. J. Biol. Macromol.* **89**, 396–405 (2016). <https://doi.org/10.1016/j.ijbiomac.2016.04.006>
38. ASTM D698: Standard test methods for laboratory compaction characteristics of soil using. *ASTM Stand. Guid.* **3**, 1–10 (2003). doi: <https://doi.org/10.1520/D1557-12.1>
39. Abbasi, S.; Rahimi, S.: Persian gum. In: Mishra, M. (ed.) *Encyclopedia of Biomedical Polymers and Polymeric Biomaterials*, pp. 5919–5928. CRC Press (2015)
40. Abbasi, S.: Challenges towards characterization and applications of a novel hydrocolloid. *Curr. Opin. Colloid Interface Sci.* **28**, 37–45 (2017)
41. Dabestani, M.; Kadkhodae, R.; Owen Philips, G.; Abbasi, S.: Persian gum: A comprehensive review on its physicochemical and functional properties. *Food Hydrocoll.* **78**, 92–99 (2018)
42. Molaei, H.; Jahanbin, K.: Structural features of a new water-soluble polysaccharide from the gum exudates of *Amygdalus scoparia* Spach (Zedo gum). *Carbohydr. Polym.* **182**, 98–105 (2018). <https://doi.org/10.1016/j.carbpol.2017.10.099>
43. Abbasi, S.: Persian Gum (*Amygdalus scoparia* Spach). In: *Emerging Natural Hydrocolloids: Rheology and Functions*. pp. 273–298 (2019)



44. Khodaei, D.; Oltrogge, K.; Hamidi-Esfahani, Z.: Preparation and characterization of blended edible films manufactured using gelatin, tragacanth gum and Persian gum. *Lwt.* **117**, 108617 (2020). <https://doi.org/10.1016/j.lwt.2019.108617>
45. Fadavi, G.; Mohammadifar, M.A.; Zargarran, A.; Mortazavian, A.M.; Komeili, R.: Composition and physicochemical properties of Zedo gum exudates from *Amygdalus scoparia*. *Carbohydr. Polym.* **101**, 1074–1080 (2014). <https://doi.org/10.1016/j.carbpol.2013.09.095>
46. Ho, L.S.; Nakarai, K.; Ogawa, Y.; Sasaki, T.; Morioka, M.: Effect of internal water content on carbonation progress in cement-treated sand and effect of carbonation on compressive strength. *Cem. Concr. Compos.* **85**, 9–21 (2018). <https://doi.org/10.1016/j.cemconcomp.2017.09.016>
47. Scrivener, K.; Snellings, R.; Lothenbach, B., et al.: *A Practical Guide to Microstructural Analysis of Cementitious Materials*. CRC Press Boca Raton, FL, USA (2016)
48. ASTM D2166: Standard Test Method for Unconfined Compressive Strength of Cohesive Soil 1. *ASTM Int.* 1–7 (2013). <https://doi.org/10.1520/D2166>
49. ASTM D3080: D3080/D3080M-11. Standard test method for direct shear test of soils under consolidated drained conditions. *ASTM Int.* (2011). <https://doi.org/10.1520/D3080>
50. ASTM D2850: Standard test method for unconsolidated-undrained triaxial compression test on cohesive soils. *ASTM International* (2007)
51. ASTM D1883: Standard test method for California bearing ratio (CBR) of laboratory-compacted soils. *ASTM International* (2016)
52. ASTM D5084: Standard test methods for measurement of hydraulic conductivity of saturated porous materials using a flexible wall permeameter. *ASTM International* (2004)
53. Ayeledeen, M.K.; Negm, A.M.; El Sawwaf, M.A.: Evaluating the physical characteristics of biopolymer/soil mixtures. *Arab. J. Geosci.* (2016). <https://doi.org/10.1007/s12517-016-2366-1>
54. Martín-Alfonso, J.E.; Cuadri, A.A.; Berta, M.; Stading, M.: Relation between concentration and shear-extensional rheology properties of xanthan and guar gum solutions. *Carbohydr. Polym.* **181**, 63–70 (2018). <https://doi.org/10.1016/j.carbpol.2017.10.057>
55. Rahimi, S.; Abbasi, S.; Sahari, M.A.; Azizi, M.H.: Characterization of an unknown exudate gum from Iran: Persian gum. In: *Electronic Conference on Innovation in Food Processing*. pp. 1–5 (2013)
56. Fadavi, G.; Mohammadifar, M.A.; Zargaran, A.; Azadnia, E.: The study of composition, molecular weight and rheological characteristics of Zedo gum exudates from *Amygdalus scoparia*. *Iran. J. Nutr. Sci. Food Technol.* **7**, 35–41 (2013)
57. Lee, S.; Im, J.; Cho, G.-C.; Chang, I.: Tri-Axial Shear Behavior of Xanthan Gum Biopolymer-Treated Sand. Presented at the March (2019)
58. Lee, M.; Im, J.; Cho, G.C.; Ryu, H.H.; Chang, I.: Interfacial shearing behavior along xanthan gum biopolymer-treated sand and solid interfaces and its meaning in geotechnical engineering aspects. *Appl. Sci.* **11**, 1–23 (2021). <https://doi.org/10.3390/app11010139>
59. Rashid, A.S.A.; Latifi, N.; Meehan, C.L.; Manahiloh, K.N.: Sustainable improvement of tropical residual soil using an environmentally friendly additive. *Geotech. Geol. Eng.* **35**, 2613–2623 (2017). <https://doi.org/10.1007/s10706-017-0265-1>
60. Soldo, A.; Miletić, M.; Auad, M.L.: Biopolymers as a sustainable solution for the enhancement of soil mechanical properties. *Sci. Rep.* **10**, 1–13 (2020). <https://doi.org/10.1038/s41598-019-57135-x>
61. Sun, Z.; Li, Z.; Qu, K.; Zhang, Z.; Niu, Y.; Xu, W.; Ren, C.: A review on recent advances in gel adhesion and their potential applications. *J. Mol. Liq.* **325**, 115254 (2021). <https://doi.org/10.1016/J.MOLLIQ.2020.115254>
62. Chang, I.; Im, J.; Cho, G.C.: Geotechnical engineering behaviors of gellan gum biopolymer treated sand. *Can. Geotech. J.* **53**, 1658–1670 (2016). <https://doi.org/10.1139/cgj-2015-0475>
63. Chang, I.; Im, J.; Prasadhi, A.K.; Cho, G.C.: Effects of Xanthan gum biopolymer on soil strengthening. *Constr. Build. Mater.* **74**, 65–72 (2015). <https://doi.org/10.1016/j.conbuildmat.2014.10.026>
64. Wu, Y.; Ding, W.; He, Q.: The gelation properties of tara gum blended with κ-carrageenan or xanthan. *Food Hydrocoll.* (2018). <https://doi.org/10.1016/j.foodhyd.2017.11.018>
65. Chen, C.; Wu, L.; Perdjion, M.; Huang, X.; Peng, Y.: The drying effect on xanthan gum biopolymer treated sandy soil shear strength. *Constr. Build. Mater.* **197**, 271–279 (2019). <https://doi.org/10.1016/j.conbuildmat.2018.11.120>
66. Li, Y.; Tanaka, T.: Phase Transitions of Gels. **22**, 243–277 (2003). <https://doi.org/10.1146/ANNUREV.MS.22.080192.001331>
67. Santamarina, J.C.; Klein, A.K.; Fam, M.A.: *Soils and Waves: Particulate Materials Behavior, Characterization and Process Monitoring*. Wiley, New York (2001)
68. Qureshi, M.U.; Chang, I.; Al-Sadarani, K.: Strength and durability characteristics of biopolymer-treated desert sand. *Geomech. Eng.* **12**, 785–801 (2017). <https://doi.org/10.12989/gae.2017.12.5.785>
69. Chang, I.; Prasadhi, A.K.; Im, J.; Shin, H.D.; Cho, G.C.: Soil treatment using microbial biopolymers for anti-desertification purposes. *Geoderma* **253–254**, 39–47 (2015). <https://doi.org/10.1016/j.geoderma.2015.04.006>
70. Mhinzi, G.S.; Mghweno, L.A.R.; Buchweishaija, J.: Intra-species variation of the properties of gum exudates from two *Acacia* species of the series *Gummiferae*. *Food Chem.* **107**, 1407–1412 (2008). <https://doi.org/10.1016/j.foodchem.2007.09.069>
71. Chang, I.; Lee, M.; Tran, A.T.P.; Lee, S.; Kwon, Y.M.; Im, J.; Cho, G.C.: Review on Biopolymer-based Soil Treatment (BPST) Technology in Geotechnical Engineering Practices, (2020)
72. Stewart, T.L.; Fogler, H.S.: Biomass plug development and propagation in porous media. *Biotechnol. Bioeng.* **72**, 353–363 (2001). [https://doi.org/10.1002/1097-0290\(20010205\)72:3%3c353::AID-BIT13%3e3.0.CO;2-U](https://doi.org/10.1002/1097-0290(20010205)72:3%3c353::AID-BIT13%3e3.0.CO;2-U)
73. Ivanov, V.; Chu, J.: Applications of microorganisms to geotechnical engineering for bioclogging and biocementation of soil in situ. *Rev. Environ. Sci. Bio/Technol.* **72**(7), 139–153 (2008). <https://doi.org/10.1007/S11157-007-9126-3>
74. Basu, D.; Misra, A.; Puppala, A.J.: Sustainability and geotechnical engineering: Perspectives and review. *Can. Geotech. J.* **52**, 96–113 (2014). <https://doi.org/10.1139/cgj-2013-0120>
75. Smitha, S.; Sachan, A.: Use of agar biopolymer to improve the shear strength behavior of sabarmati sand. *Int. J. Geotech. Eng.* **10**, 387–400 (2016). <https://doi.org/10.1080/19386362.2016.1152674>
76. Guo, L.: Investigation of soil stabilization using biopolymers. (2014). <https://dr.lib.iastate.edu/handle/20.500.12876/28096>
77. Alsanad, A.: Novel biopolymer treatment for wind induced soil erosion. (2011). <https://hdl.handle.net/2286/R.I.9118>
78. Yosefi, F.; Abbasi, S.; Ezatpanah, H.: Effect of Persian gum concentration, oil content, whey protein concentrate, and pH on the stability of emulsions prepared by ultrasonic homogenizer. *Res. Innov. Food Sci. Technol.* **1**, 199–218 (2012)
79. Latifi, N.; Horpibulsuk, S.; Meehan, C.L.; Majid, M.Z.A.; Rashid, A.S.A.: Xanthan gum biopolymer: an eco-friendly additive for stabilization of tropical organic peat. *Environ. Earth Sci.* (2016). <https://doi.org/10.1007/s12665-016-5643-0>
80. Arab, M.G.; Mousa, R.A.; Gabr, A.R.; Azam, A.M.; El-Badawy, S.M.; Hassan, A.F.: Resilient behavior of sodium alginate-treated cohesive soils for pavement applications. *J. Mater. Civ. Eng.* **31**, 04018361 (2019). [https://doi.org/10.1061/\(ASCE\)MT.1943-5533.0002565](https://doi.org/10.1061/(ASCE)MT.1943-5533.0002565)
81. Mahmood, M.S.; Akhtarpour, A.; Alali, A.A.A.: Mechanical behavior of dam foundation with vertical sand drain, case study:

- Sombar Dam. *J. Eng. Technol. Sci.* (2019). <https://doi.org/10.5614/j.eng.technol.sci.2019.51.3.6>
82. Yang, L.; Yang, Y.; Chen, Z.; Guo, C.; Li, S.: Influence of super absorbent polymer on soil water retention, seed germination and plant survivals for rocky slopes eco-engineering. *Ecol. Eng.* (2014). <https://doi.org/10.1016/j.ecoleng.2013.10.019>
83. Saadatkah, N.; Carillo Garcia, A.; Ackermann, S.; Leclerc, P.; Latifi, M.; Samih, S.; Patience, G.S.; Chaouki, J.: *Experimental methods in chemical engineering: thermogravimetric analysis—TGA* (2020)